JOURNAL OF VIROLOGY, Dec. 1999, p. 10371–10376 Vol. 73, No. 12
0022-538X/99/$04.00+0

Dynamin Is Required for Recombinant Adeno-Associated Virus Type 2 Infection

DONGSHENG DUAN,[1,2] QIANG LI,[1] AIMEE W. KAO,[3] YONGPING YUE,[1] JEFFREY E. PESSIN,[3] AND JOHN F. ENGELHARDT[1,2,4]*

Department of Anatomy and Cell Biology,[1] Department of Internal Medicine,[4] Center for Gene Therapy,[2] and Department of Physiology and Biophysics,[3] College of Medicine, The University of Iowa, Iowa City, Iowa 52242

Received 1 June 1999/Accepted 3 September 1999

Recombinant adeno-associated virus (rAAV) vectors for gene therapy of inherited disorders have demonstrated considerable potential for molecular medicine. Recent identification of the viral receptor and coreceptors for AAV type 2 (AAV-2) has begun to explain why certain organs may demonstrate higher efficiencies of gene transfer with this vector. However, the mechanisms by which AAV-2 enters cells remain unknown. In the present report, we have examined whether the endocytic pathways of rAAV-2 are dependent on dynamin, a GTPase protein involved in clathrin-mediated internalization of receptors and their ligands from the plasma membrane. Using a recombinant adenovirus expressing a dominant-inhibitory form of dynamin I (K44A), we have demonstrated that rAAV-2 infection is partially dependent on dynamin function. Overexpression of mutant dynamin I significantly inhibited AAV-2 internalization and gene delivery, but not viral binding. Furthermore, colocalization of rAAV and transferrin in the same endosomal compartment provides additional evidence that clathrin-coated pits are the predominant pathway for endocytosis of AAV-2 in HeLa cells.

Recombinant adeno-associated virus (rAAV) has gained increasing popularity for gene therapy of numerous organs. As the field has matured in this area, it has become obvious that striking differences in efficiency of transduction to various tissues exist for rAAV. For example, rAAV-mediated gene transfer to muscle and brain is quite efficient, while transduction in the lung is not (2, 7, 9, 11, 14, 19, 28). Although studies have related these differences in tissue transduction to the phosphorylation state of certain cellular factors, such as the single-stranded DNA binding protein (19), which may control the transformation of the single-stranded AAV genome into expressible double-stranded forms, others have suggested that the abundance of the AAV type 2 (AAV-2) receptor and coreceptors may be at the heart of differing transduction efficiencies. These studies have suggested that heparan sulfate proteoglycan (HSPG) is the primary receptor for AAV-2 binding (23), while fibroblast growth factor receptor type 1 (FGFR-1) (20) and αVβ5 integrin (22) are coreceptors for efficient binding and internalization of AAV-2 virus. Additionally, studies of the airway have suggested that alternative pathways of viral entry independent of HSPG, FGFR-1, and αVβ5 integrin may occur from the apical membrane following UV-induced rAAV transduction (9). Despite these observations, little is known regarding the mechanism(s) of endocytosis of rAAV-2 in mammalian cells. Knowledge in this area may aid in identifying alternative approaches to enhance viral entry into cell types for which transduction is normally low.

Two classical mechanisms are involved in the endocytosis of foreign substances into eukaryotic cells. These include phagocytosis of large molecules and receptor-mediated endocytosis through clathrin-coated pits (16). Critical aspects of clathrin-mediated endocytosis were first identified in *Drosophila* following isolation of the temperature-sensitive paralytic mutant, *Shibire*. The *shibire* gene product is an ortholog to mammalian dynamin I. Mutations in the *shibire* gene result in pleiotropic dysfunction of endocytosis in *Drosophila* cells (5). Subsequently, it was demonstrated that the GTPase activity of the dynamin is also necessary for mammalian cell endocytosis (21). Specifically, oligomerization of dynamin into a ring structure is required for the formation of clathrin-coated vesicles and subsequent pinching of coated pits from the cell membrane. A substitution mutation of lysine to alanine (K44A) in the GTP binding site results in a dominant-negative dynamin I mutant (25). This mutant form of dynamin has been extensively used to demonstrate the importance of clathrin-mediated endocytosis for transferrin, epidermal growth factor, and insulin through their respective receptors (4, 5, 13, 26). Interestingly, recent studies indicate that internalization of adenovirus also requires dynamin (18, 27). Since adenovirus is a helper virus for productive AAV infection and these two viruses both appear to use αVβ5 integrin as a coreceptor, we reasoned that clathrin-mediated endocytosis might also mediate rAAV-2 entry and infection in mammalian cells. To this end, we have evaluated the importance of dynamin-dependent endocytosis of AAV-2 in HeLa cells by using a recombinant adenovirus (rAd) expressing the dominant-negative mutant form (K44A) of dynamin I.

MATERIALS AND METHODS

Production of rAAV-2 and rAd. rAAV-2 was generated by using a previously described *cis*-acting plasmid (pCisAV.GFP3ori) (7). The recombinant viral stock was generated by cotransfection of 293 cells with pCisAV.GFP3ori and pRep/Cap and coinfection with recombinant Ad.CMVlacZ according to a previously published protocol (6). AAV-2 was purified through three rounds of isopycnic cesium chloride density centrifugation ($\rho = 1.4$) followed by heating at 58°C for 60 min to inactivate all contaminant helper adenovirus (6). Typically, this preparation gave approximate AAV titers of 5×10^{12} DNA molecules/ml and 5×10^{8} green fluorescent protein (GFP)-expressing units/ml. Recombinant viral titers were assessed by slot blotting and quantified against pCisAV.GFP3ori controls for DNA particles. Functional transducing units were quantified by GFP transgene expression in 293 cells. The absence of helper adenovirus was confirmed by histochemical staining of rAAV-infected 293 cells for β-galactosidase, and no rAd was found in 10^{10} particles of purified rAAV stocks. The absence of significant wild-type AAV contamination was confirmed by immunocytochemical staining of rAAV-rAd coinfected 293 cells with anti-Rep antibodies. These studies had a sensitivity of 1 wild-type AAV in 10^{10} rAAV particles and dem-

* Corresponding author. Mailing address: Department of Anatomy and Cell Biology, University of Iowa, College of Medicine, 51 Newton Rd., Room 1-111 BSB, Iowa City, IA 52242-1109. Phone: (319) 335-7753. Fax: (319) 335-7198. E-mail: john-engelhardt@uiowa.edu.

onstrated an absence of Rep staining compared to that in pRep/Cap plasmid-transfected controls. The rAd was amplified by infecting 80% confluent 293 cells in Dulbecco's modified Eagle's medium (DMEM) containing 2% fetal bovine serum (FBS). The virus was harvested at 32 h postinfection when full cytopathic effect was reached. The amplified virus was subsequently purified according to a previously published protocol (10). Functional recombinant virus titers for Ad.CMVLacZ, Ad.K44Adynamin, and Ad.RSVGFP, were assessed on HeLa cells by expression of β-galactosidase, hemagglutinin (HA)-tagged dynamin, and GFP fluorescence, respectively. DNA particle titers were also assessed by slot blot hybridization with plasmid DNA standards.

Production of ^{35}S-labeled rAAV and Cy3-labeled rAAV. ^{35}S labeling of rAV.GFP3ori capsid was performed according to a previously published protocol with modifications (17). Briefly, 10 150-mm-diameter plates of 80% confluent 293 cells were infected with Ad.LacZ (5 PFU/cell) for 70 min, followed by calcium phosphate transfection of pCisAV.GFP3ori (250 μg) and pRepCap (750 μg). Cells were incubated for an additional 9 h, at which time, the medium was changed to 2% FBS–methionine-free DMEM for 60 min. The medium was then changed again to labeling medium containing 10 mCi of [^{35}S]methionine (specific activity, 43.5 TBq/mmol; NEN Dupont) per 200 ml of 2% FBS–methionine-free DMEM (final concentration, 1.85 MBq/ml), and cells were pulsed for 2 h at 37°C. Following labeling, L-methionine was added back to a final concentration of 30 mg/liter. ^{35}S-labeled virus was harvested at 34 h posttransfection and purified by isopycnic cesium chloride ultracentrifugation as described above. Finally, virus was dialyzed against five changes of HEPES-buffered saline (pH 7.8) at 4°C. Typical specific activities of labeled virus were 9×10^{-6} cpm/particle. Cyanine-3 (Cy3) fluorophore-labeled rAAV was produced by conjugating bifunctional sulfoindocyanin 3 dye (FluoroLink-Ab Cy3 labeling kit; Amersham-Life Sciences, Arlington Heights, Ill.) to isopycnic cesium chloride-purified AV.GFP3ori. The reaction was performed according to the manufacturer's instructions with modifications. Briefly, the rAAV stock virus AV.GFP3ori (4×10^{12} viral particles in 5% glycerol–HEPES buffer) was thawed on ice and resuspended in 1 ml of phosphate-buffered saline (PBS). The virus was then cleared by centrifugation and concentrated to 50 μl in a Centricon-100 (Millipore Corporation, Bedford, Mass.). The concentrated virus was resuspended in 1 ml of 0.1 M sodium carbonate buffer (pH 9.3) and incubated at room temperature for 30 min with 50 nmol of Cy3 dye by adding 50 μl of a 1-nmol/μl Cy3 stock solution in the same sodium carbonate buffer. The conjugation reaction was stopped by adding 1 ml of 10 mM Tris (pH 8.0) to the solution. To prevent the degradation of labeled virus, the pH of the labeling reaction was neutralized down to 8.0 with 1 N HCl immediately after labeling. Labeled virus was then dialyzed against five changes of PBS (molecular mass cutoff, 10,000 Da; Gibco BRL Life Technologies, Inc., Gaithersburg, Md.) at 4°C over the course of 2 days. Finally, the Cy3-labeled virus was concentrated with a Centricon-30 (Millipore Corporation) to a final concentration of 4×10^8 particles/μl. On average, 3.53 Cy3 dye molecules were conjugated to each viral particle. The dye/particle ratio was calculated based on the Southern blot determination of viral particles and the extinction coefficient of Cy3 dye ($\varepsilon_{580} = 1.5 \times 10^5\ M^{-1}\ cm^{-1}$) to determine the number of Cy3 molecules. No significant decrease in infectious titer on 293 cells was observed in labeled viral stocks compared with the titer of mock-labeled virus.

Indirect immunofluorescent detection of HA-tagged Ad.K44Adynamin. Localization of HA-tagged K44A mutant dynamin I was performed with a monoclonal antibody which specifically recognizes the influenza virus HA epitope (clone 12CA5; Boehringer Mannheim Corp., Indianapolis, Ind.). Forty-eight hours post-rAd infection, cells were fixed in 4% paraformaldehyde for 10 min at room temperature and permeabilized in 0.2% Triton X-100 for 10 min at room temperature. The samples were then blocked in 20% goat serum–PBS for 30 min, followed by incubation in a 1:100 dilution of fluorescein isothiocyanate (FITC)-conjugated 12CA5 monoclonal antibody for 90 min. The cells were washed in 1.5% goat serum–PBS for 8 min three times. Finally, cells were mounted with Citifluor antifadent (glycerol-PBS solution; UKC Chem. Lab, Canterbury, United Kingdom) prior to imaging by indirect immunofluorescence.

Southern blot detection of AAV-2 binding and entry in HeLa cells. Dynamin I-dependent endocytosis of rAAV DNA in HeLa cells was assayed following infection with Ad.LacZ or Ad.K44Adynamin (multiplicity of infection [MOI] = 5,000 particles/cell) 48 h prior to rAAV infection with AV.GFP3ori (MOI = 1,000 particles/cell) at 4°C for 1 h to assess binding. Following binding, internalization was assessed by continuing incubations in the presence of virus at 37°C for 3, 6, and 24 h. Viral DNA was extracted according to a modified Hirt protocol, and Southern blots were performed with Hybond N+ nylon membrane (Amersham) (6). The 1.6-kb single-stranded AAV viral genome was detected with a transgene-specific enhanced GFP (EGFP) probe at 10^6 cpm/ml and washed at a stringency of 0.1× SSC (1× SSC is 0.15 M NaCl plus 0.015 M sodium citrate)–0.1% sodium dodecyl sulfate (SDS) at 60°C for 20 min twice. The virus attached to the cell surface was removed by trypsinization with a buffer containing 0.5% trypsin–5.3 mM EDTA at 37°C for 5 min, followed by a wash with ice-cold PBS twice. The externally bound AAV virus was determined by the intensity of the 1.6-kb viral genome band in Hirt DNA extracted from cells infected at 4°C for 60 min. The internalized virus was determined by the intensity of the 1.6-kb viral genome band in Hirt DNA extracted from trypsinized cells after infection at 37°C for 3, 6, and 24 h.

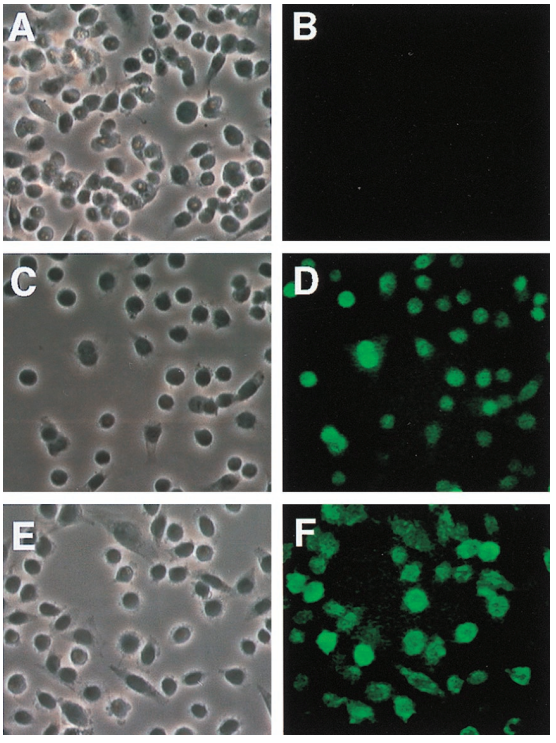

FIG. 1. Immunofluorescent detection of the K44A dominant-negative dynamin I mutant in HeLa cells following rAd-mediated expression. Fifty percent confluent HeLa cells were infected with rAd expressing β-galactosidase (A and B), HA-tagged IκB (C and D), or HA-tagged K44A dynamin I mutant (E and F) at an MOI of 1,000 particles/cell for 48 h in 2% FBS–DMEM. Cells were then fixed in 4% paraformaldehyde for 10 min and permeabilized in 0.2% Triton X-100 for 10 min. After blocking with 20% goat serum for 30 min, HA epitope was detected with a 1:100 dilution of mouse monoclonal anti-HA FITC-conjugated antibody (clone 12CA5; Boehringer Mannheim Corp.) Panels A, C, and E are Nomarski photomicrographs of the FITC fluorescent fields shown in panels B, D, and F, respectively.

RESULTS

rAAV transduction in HeLa cells is inhibited by mutant dynamin I expression. To evaluate the involvement of dynamin I in the endocytic pathways of AAV-2, we utilized a rAd expressing K44A mutant dynamin I which has been previously described (4, 13). This K44A mutant dynamin I is also tagged with an influenza virus HA epitope (25). To demonstrate rAd-mediated expression of the dynamin I K44A mutant in HeLa cells, we performed immunofluorescent staining with a monoclonal antibody against the HA epitope (Fig. 1). As a positive control for immunofluorescent staining, cells were also evaluated following infection by another HA-tagged adenovirus (rAd.MIκB) which has been well characterized (12). No background staining was observed in non-HA-tagged Ad.LacZ-infected cells. Similar to previous reports with other cell lines, such as 3T3L1 adipocytes and rat H4IIE hepatocytes (4, 13), a significant level of K44A mutant dynamin I was expressed in HeLa cells at 48 h following rAd infection.

Since adenovirus internalization is significantly repressed by overexpression of mutant K44A dynamin I in HeLa cells (18, 27), we have included recombinant Ad.CMVGFP as a positive control for functional inhibition of endogenous dynamin in our experiments with AAV-2 (Fig. 2). As was expected, adenovirus-mediated expression of K44A dynamin I 48 h prior to infection with a second GFP-expressing adenovirus inhibited GFP expression by fourfold. To evaluate the effects of K44A

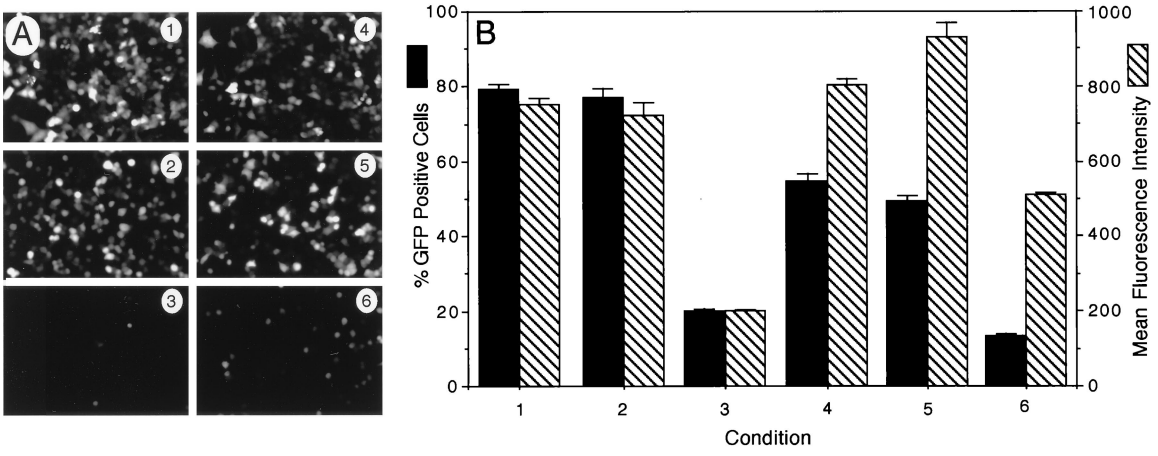

FIG. 2. Expression of K44A dynamin I mutant inhibits rAAV-2-mediated gene transfer in HeLa cells. The effects of K44A dynamin I expression on the transduction efficiency of rAd (Ad.GFP) or rAAV (AV.GFP3ori) were evaluated. Eighty percent confluent HeLa cells were first infected with rAd expressing either K44A dynamin I or LacZ (MOI = 5,000 particles/cell) 48 h prior to infection with GFP-expressing rAd (MOI = 1,000 particles/cell) and rAAV (MOI = 1,000 particles/cell). Control experiments were also performed in which HeLa cells were infected with either Ad.GFP or AV.GFP3ori alone (both at MOI = 1,000 particles/cell). GFP transgene expression was detected at 24 h postinfection by either indirect fluorescent microscopy (A) or by flow cytometric analysis (B). Conditions in panels A and B are indicated numerically as follows: 1, infection with Ad.GFP alone; 2, preinfection with Ad.LacZ followed by superinfection with Ad.GFP; 3, preinfection with Ad.K44Adynamin followed by superinfection with Ad.GFP; 4, infection with AV.GFP3ori alone; 5, preinfection with Ad.LacZ followed by superinfection with AV.GFP3ori; 6, preinfection with Ad.K44Adynamin followed by superinfection with AV.GFP3ori. The data represent the mean ± standard error of three independent experiments.

dynamin I on AAV-2 transduction, HeLa cells were infected with either Ad.LacZ or Ad.K44Adynamin for 48 h prior to infection with an rAAV vector (AV.GFP3ori) encoding the GFP (7). In these studies, adenovirus-mediated K44A dynamin I expression reduced rAAV-mediated GFP gene expression by 3.7-fold (Fig. 2). Expression of K44A dynamin appeared to inhibit both the percentage of GFP-expressing cells as well as the relative mean fluorescent intensity of GFP-positive cells (Fig. 2B). In contrast, prior infection with Ad.LacZ had no effect on rAAV-mediated gene expression. Similar to what has been described for adenovirus, mutant dynamin I expression only partially inhibited rAAV transduction. This partial effect was not due to inefficient infection with adenovirus, since at the current MOIs of Ad.LacZ and Ad.K44Adynamin (MOI = 5,000 particles/cell) used for our experiment, 100% of the cells were targeted according to LacZ staining (data not shown) and immunofluorescent staining of HA-tagged dynamin (Fig. 1). Therefore, it is possible that either overexpression of the dynamin I mutant does not provide complete functional inhibition of dynamin multimer formation in HeLa cells, or there may exist alternative dynamin-independent pathways for AAV entry into HeLa cells.

Internalization but not viral binding is blocked by the K44A dynamin I mutant. To further clarify the stage of viral infection potentially blocked by overexpression of dominant-negative mutant dynamin I, we next studied whether AAV viral binding and/or internalization was responsible for the observed decreased transduction. As was described above, HeLa cells were first infected with either the Ad.LacZ or Ad.K44Adynamin mutant or mock infected without adenovirus. Forty-eight hours after adenovirus infection, HeLa cells were superinfected with AV.GFP3ori at 4°C for 60 min to determine the binding of rAAV virus. Low-molecular-weight Hirt DNA was harvested from these cells, and rAAV attached to the cell surface was detected by Southern blotting with an EGFP transgene-specific probe. As shown in Fig. 3 (lanes 4 to 6), no AAV DNA was detected when the cells were first trypsinized before Hirt DNA extraction. This suggested that no rAAV virus was internalized into cells during the 4°C incubation period. In contrast, following 4°C infections with rAAV, equivalent amounts of rAAV

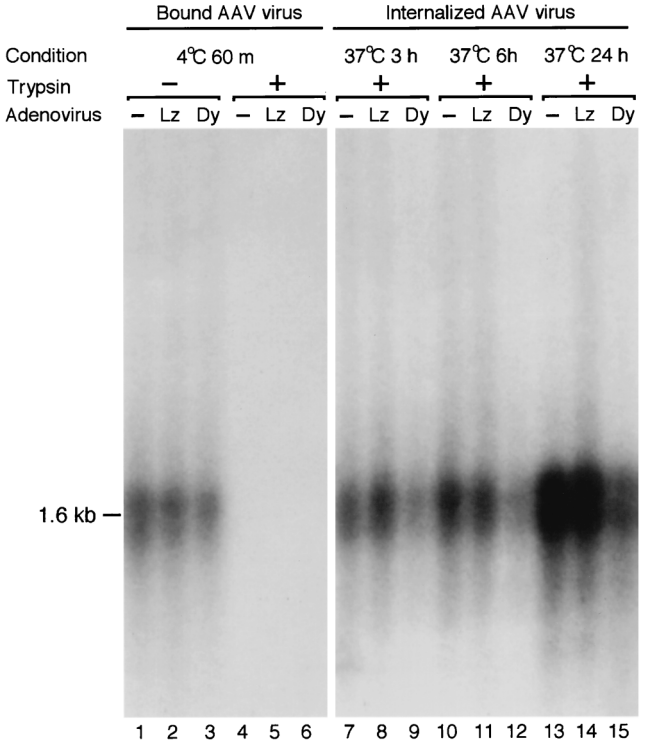

FIG. 3. Southern blot analysis of rAAV DNA entry into HeLa cells. HeLa cells were preinfected with either Ad.LacZ (Lz) or Ad.K44Adynamin (Dy) at an MOI of 5,000 particles/cell for 48 h. A control set of HeLa cells which were not preinfected with rAd (−) were also included in the study to assess for the baseline binding and internalization of rAAV in the absence of any modifications. The binding of rAAV to HeLa cells was determined by AV.GFP3ori infection (MOI = 1,000 particles/cell) at 4°C for 1 h followed by Hirt DNA analysis on Southern blots against ^{32}P-labeled EGFP DNA probes (lanes 1, 2, and 3). Treatment of cells with trypsin prior to Hirt DNA extraction removed all cell-surface-bound rAAVs (lanes 4, 5, and 6). The extent of viral DNA endocytosis was determined by the fraction of trypsin-resistant internalized viral genome at 37°C for the various incubation times indicated. The 1.6-kb bands represent single-stranded rAAV DNA.

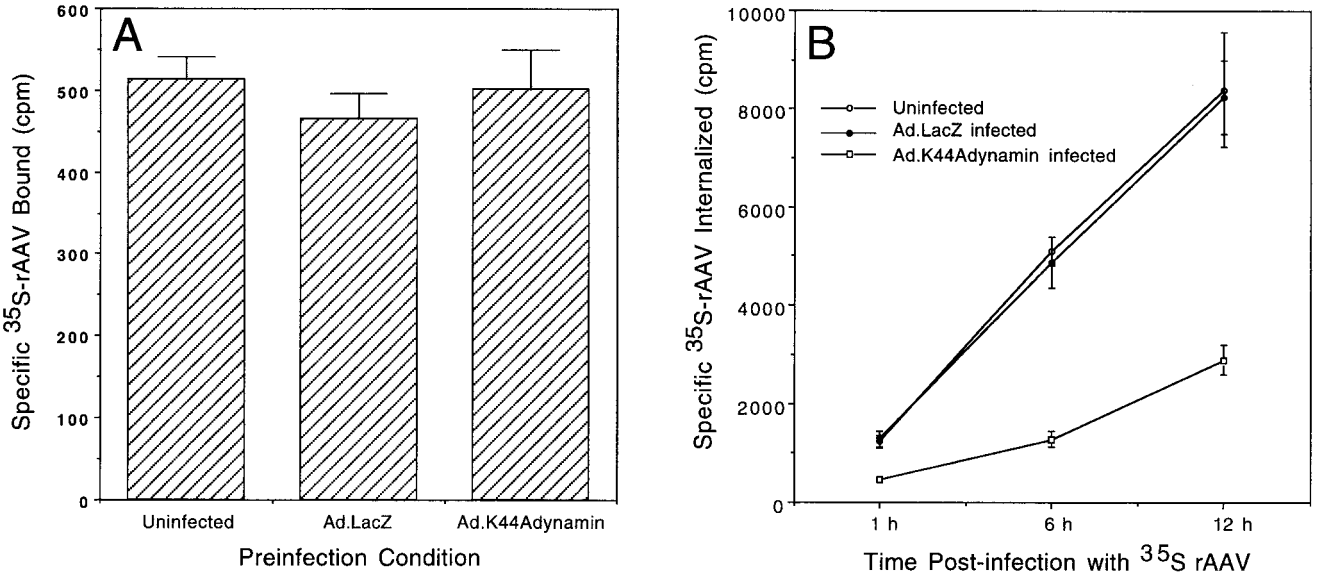

FIG. 4. Viral internalization, but not binding, is affected by overexpression of the K44A dynamin I mutant. HeLa cells (10^6) were preinfected with either Ad.LacZ or Ad.K44Adynamin (MOI = 5,000 particles/cell) for 48 h. Uninfected cells were also included as controls for the baseline binding and internalization in the absence of adenovirus preinfection. To quantify rAAV binding (A), HeLa cells were then infected with 9×10^4 cpm of ^{35}S-labeled rAAV at 4°C for 1 h. After washing in ice-cold PBS three times, cells were lysed in 1× RIAP buffer (50 mM Tris 7.5, 150 mM NaCl, 1% Triton X-100, 1% Na-deoxycholate, 0.1% SDS), and radioactivity was quantified in a scintillation counter. Panel B depicts the net internalized ^{35}S-labeled virus at 1, 6, and 12 h after rAAV infection. In this set of experiments, surface-bound virus was removed by trypsinization and PBS washing prior to cell lysis in 1× RIAP buffer and quantification of radioactivity. The data are the mean ± standard error of three independent samples.

DNA were detected in Hirt DNAs from nontrypsinized cells preinfected with Ad.LacZ and Ad.K44Adynamin or in untreated controls (Fig. 3, lane 1 to 3). These data indicate that rAAV binding to the cell surface was not significantly perturbed by overexpression of mutant dynamin I or preinfection with adenovirus. Immediately after binding of rAAV at 4°C, cells were also transferred to 37°C to promote internalization of the rAAV. In order to compare the internalization of rAAV virus in K44A dominant mutant-expressing cells, cellular Hirt DNA was harvested at 3, 6, and 24 h post-rAAV infection. Cell surfaces were stripped of uninternalized rAAV by treatment with trypsin immediately prior to Hirt DNA extraction, so that only internalized virus was compared. Although a small amount of rAAV was able to enter mutant dynamin I-expressing cells as early as 3 h post-rAAV infection (Fig. 3, lane 9), the amount of virus that was internalized in Ad.LacZ-infected or noninfected cells was much higher at all time points studied. These data strongly suggest that mutant dynamin expression can significantly inhibit rAAV endocytosis in HeLa cells and substantiate earlier findings of reduced transgene expression in the presence of this mutant. Similarly, residual rAAV DNA endocytosis in the presence of overexpressed mutant dynamin I suggests that a small amount of functional ring or spiral structures can still be formed from self-assembly of endogenous dynamin II molecules in HeLa cells. Alternatively, dynamin-independent mechanisms of viral entry may also exist, albeit at lower levels.

To confirm the results from the viral genome analysis presented above and to provide more direct and quantitative evidence for the involvement of dynamin in AAV endocytosis, we compared the attachment and internalization of ^{35}S-labeled AAV in the absence and presence of the K44Adynamin I mutant. Similar to conditions in other sets of experiments (Fig. 2 and 3), HeLa cells were also preinfected with the Ad.LacZ or Ad.K44Adynamin I mutant for 48 h prior to ^{35}S-AAV infection. As shown in Fig. 4A, no difference in rAAV binding was observed as a result of infection with either Ad.LacZ or Ad.K44Adynamin. Together with the results in Fig. 3, we conclude that the inhibition of rAAV-mediated gene transfer by the dynamin I mutant was not due to inhibition on viral attachment. Quantification of GFP transgene-expressing cells by fluorescence-activated cell sorting suggested that K44A dynamin I overexpression inhibited rAAV transduction by 3.7-fold (Fig. 2B). Consistent with this finding, internalization rates of ^{35}S-labeled rAAV in Ad.K44Adynamin-preinfected cells (229 cpm/h or 25 viral particles cell^{-1} h^{-1}) were threefold lower than that observed in cells preinfected with Ad.LacZ (672 cpm/h or 74 viral particles cell^{-1} h^{-1}) or mock-infected control cells (690 cpm/h or 76 viral particles cell^{-1} h^{-1}) (Fig. 4B). Taken together, these findings have demonstrated a strong correlation between decreased rAAV transduction and reduced viral internalization in mutant dynamin I-expressing HeLa cells. Based on the fact that dynamin is an essential component of clathrin-mediated endocytosis (15), our data suggest that the clathrin-coated pit might be the predominant pathway for the infectious entry of rAAV.

Internalization of rAAV shares the same endocytic compartment with transferrin. To further clarify the involvement of clathrin-coated pits in rAAV endocytosis, we have used Cy3-AAV virions to directly visualize viral endocytosis in HeLa cells. Internalization of transferrin has been known as a classic example of endocytosis through clathrin-coated pits. Therefore, FITC-transferrin was used to mark the clathrin-dependent endocytic pathway. In these experiments, Cy3-AAV and FITC-transferrin were initially bound to the surface of HeLa cells by incubation at 4°C for 60 min. Endocytosis of virus and transferrin was visualized after shifting the incubation temperature of cells to 37°C for 10 min. As shown in Fig. 5, the majority of the Cy3-AAV particles colocalize with FITC-transferrin in the same endocytic vesicles. This piece of data pro-

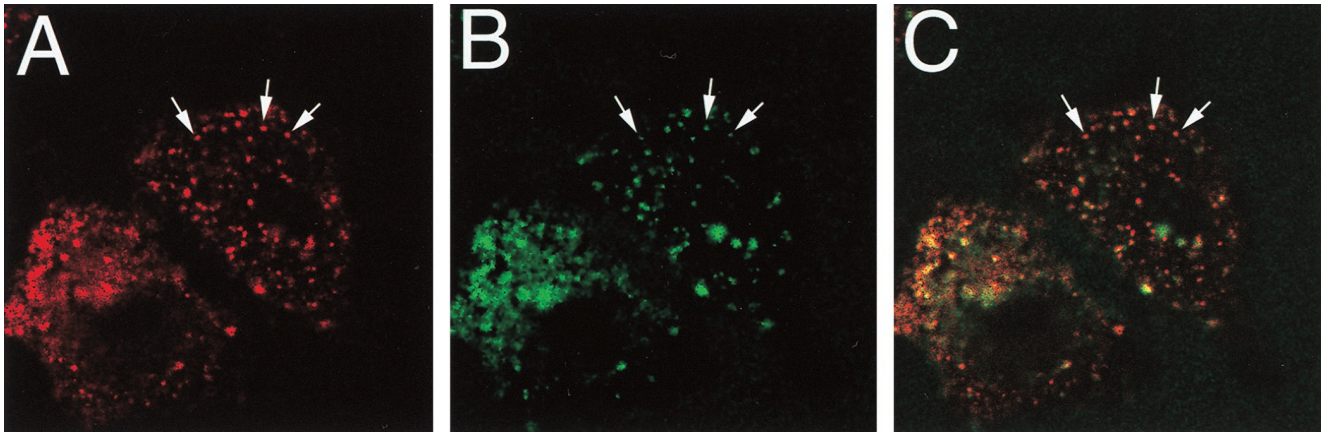

FIG. 5. Colocalization of Cy3-labeled rAAV and fluorescein-labeled transferrin. To directly evaluate endocytosis of rAAV, 4×10^3 HeLa cells grown on glass slides were precooled at 4°C for 10 min and subsequently infected with 4×10^8 particles of Cy3-labeled rAAV at 4°C for 1 h (MOI = 100,000) in the presence of 15-μg/ml FITC-transferrin. Endocytosis of rAAV and FITC-transferrin was initiated by shifting cells to 37°C for 10 min. After extensive washing in ice-cold PBS, cells were fixed in 4% paraformaldehyde and mounted with Citifluor antifadent. Confocal fluorescence photomicrographs were taken for rAAV (A), transferrin (B), and combined FITC-rhodamine (C) channels. Arrows mark the colocalization of Cy3-rAAV and transferrin within the same endosome compartment.

vided additional support that rAAV endocytosis takes places through clathrin-coated pits.

DISCUSSION

Because rAAV is a nonpathogenic virus capable of transducing a broad range of cell types both in vitro and in vivo, this vector system has attracted tremendous interest in the field of gene therapy. Significant progress has been made in understanding the molecular events involved in viral transduction, such as viral second-strand synthesis and the formation of circular transduction intermediates. However, knowledge regarding the cellular endocytic trafficking of this virus remains elusive. For example, fully differentiated airway cells have been shown to lack AAV-2 receptor (HSPG) and coreceptors (including FGFR-1 and αVβ5 integrin) on their mucosal surface (8). Although the abundance of the receptor and coreceptor indeed plays a role in higher-level transduction following basolateral compared to apical infection in the airway, additional pathways of viral binding and entry from the apical surface also seem to exist. In support of this notion, UV irradiation has been shown to augment rAAV transduction from the apical membrane despite a lack of HSPG AAV-2 receptor and coreceptors on this surface (9). In the present report, we have begun to address the role of receptor-mediated endocytosis during rAAV infection.

The involvement of dynamin in AAV-2 infection and the colocalization of rAAV with transferrin during endocytosis suggest that clathrin-dependent receptor-mediated endocytosis is the predominant, but not the exclusive, pathway for rAAV entry into HeLa cells. The lack of complete inhibition of rAAV endocytosis by K44A dynamin I suggests two possibilities. First, unidentified dynamin-independent pathways might be involved in infectious entry of rAAV-2. Second, the K44A dynamin I mutant may not effectively inhibit all dynamin-dependent receptor-mediated endocytic processes in HeLa cells. Three closely related mammalian dynamin isoforms (dynamins I, II, and III) have recently been isolated. Dynamin II is ubiquitously expressed in most cell types, including HeLa cells. In contrast, dynamin I is expressed only in neuronal cells, and dynamin III is preferentially expressed in testes, neurons, and the lung (3, 24). Although many studies have used the neuronal isoform dynamin I mutant (K44A) to study receptor-mediated endocytosis in nonneuronal cells (4, 13, 18, 27), different dynamin isoforms do seem to have redundant, but also distinct, functions in different cell types. For example, both dynamin I (K44A) and dynamin II (K44A) mutants are strong inhibitors of receptor-mediated endocytosis in both HeLa and polarized MDCK cells. However, the dynamin II (K44A) mutant is more potent than the dynamin I mutant in HeLa cells. In MDCK cells, dynamin I appears to be more important for apical endocytosis, while dynamin II is preferred for basolateral endocytosis (1). While additional studies are needed to fully understand how many pathways of rAAV entry exist in various cell types, our studies have provided a direct link between dynamin-dependent receptor-mediated internalization of rAAV and its infection in HeLa cells.

ACKNOWLEDGMENTS

This work was supported by National Institutes of Health grant HL51887 (J.F.E.) and pilot grant (D.D.) of the Gene Therapy Center for Cystic Fibrosis and Other Genetic Diseases funded by the National Institutes of Health and Cystic Fibrosis Foundation (DK54759 [J.F.E.]).

REFERENCES

1. **Altschuler, Y., S. M. Barbas, L. J. Terlecky, K. Tang, S. Hardy, K. E. Mostov, and S. L. Schmid.** 1998. Redundant and distinct functions for dynamin-1 and dynamin-2 isoforms. J. Cell Biol. **143:**1871–1881.
2. **Bennett, J., D. Duan, J. F. Engelhardt, and A. M. Maguire.** 1997. Real-time, noninvasive in vivo assessment of adeno-associated virus-mediated retinal transduction. Investig. Ophthalmol. Vis. Sci. **38:**2857–2863.
3. **Cao, H., F. Garcia, and M. A. McNiven.** 1998. Differential distribution of dynamin isoforms in mammalian cells. Mol. Biol. Cell **9:**2595–2609.
4. **Ceresa, B. P., A. W. Kao, S. R. Santeler, and J. E. Pessin.** 1998. Inhibition of clathrin-mediated endocytosis selectively attenuates specific insulin receptor signal transduction pathways. Mol. Cell. Biol. **18:**3862–3870.
5. **Damke, H., T. Baba, D. E. Warnock, and S. L. Schmid.** 1994. Induction of mutant dynamin specifically blocks endocytic coated vesicle formation. J. Cell Biol. **127:**915–934.
6. **Duan, D., K. J. Fisher, J. F. Burda, and J. F. Engelhardt.** 1997. Structural and functional heterogeneity of integrated recombinant AAV genomes. Virus Res. **48:**41–56.
7. **Duan, D., P. Sharma, J. Yang, Y. Yue, L. Dudus, Y. Zhang, K. J. Fisher, and J. F. Engelhardt.** 1998. Circular intermediates of recombinant adeno-associated virus have defined structural characteristics responsible for long-term episomal persistence in muscle tissue. J. Virol. **72:**8568–8577.
8. **Duan, D., Y. Yue, and J. F. Engelhardt.** 1999. Polarity influences the efficiency of recombinant adeno-associated virus infection in differentiated airway epithelia. Hum. Gene Ther. **10:**1553–1557. (Letter.)
9. **Duan, D., Y. Yue, Z. Yan, P. B. McCray, and J. F. Engelhardt.** 1998. Polarity

influences the efficiency of recombinant adeno-associated virus infection in differentiated airway epithelia. Hum. Gene Therapy **9:**2761–2776.
10. **Engelhardt, J. F., R. H. Simon, Y. Yang, M. Zepeda, S. Weber-Pendleton, B. Doranz, M. Grossman, and J. M. Wilson.** 1993. Adenovirus-mediated transfer of the CFTR gene to lung of nonhuman primates: biological efficacy study. Hum. Gene Ther. **4:**759–769.
11. **Fisher, K. J., G.-P. Gao, M. D. Weitzman, R. DeMatteo, J. F. Burda, and J. M. Wilson.** 1996. Transduction with recombinant adeno-associated virus for gene therapy is limited by leading-strand synthesis. J. Virol. **70:**520–532.
12. **Iimuro, Y., T. Nishiura, C. Hellerbrand, K. E. Behrns, R. Schoonhoven, J. W. Grisham, and D. A. Brenner.** 1998. NFkappaB prevents apoptosis and liver dysfunction during liver regeneration. J. Clin. Investig. **101:**802–811.
13. **Kao, A. W., B. P. Ceresa, S. R. Santeler, and J. E. Pessin.** 1998. Expression of a dominant interfering dynamin mutant in 3T3L1 adipocytes inhibits GLUT4 endocytosis without affecting insulin signaling. J. Biol. Chem. **273:** 25450–25457.
14. **Kaplitt, M. G., P. Leone, R. J. Samulski, X. Xiao, D. W. Pfaff, K. L. O'Malley, and M. J. During.** 1994. Long-term gene expression and phenotypic correction using adeno-associated virus vectors in the mammalian brain. Nat. Genet. **8:**148–154.
15. **Marsh, M., and H. T. McMahon.** 1999. The structural era of endocytosis. Science **285:**215–220.
16. **Mellman, I.** 1996. Endocytosis and molecular sorting. Annu. Rev. Cell Dev. Biol. **12:**575–625.
17. **Mizukami, H., N. S. Young, and K. E. Brown.** 1996. Adeno-associated virus type 2 binds to a 150-kilodalton cell membrane glycoprotein. Virology **217:** 124–130.
18. **Pickles, R. J., D. McCarty, H. Matsui, P. J. Hart, S. H. Randell, and R. C. Boucher.** 1998. Limited entry of adenovirus vectors into well-differentiated airway epithelium is responsible for inefficient gene transfer. J. Virol. **72:** 6014–6023.
19. **Qing, K., B. Khuntirat, C. Mah, D. M. Kube, X.-S. Wang, S. Ponnazhagan, S. Zhou, V. J. Dwarki, M. C. Yoder, and A. Srivastava.** 1998. Adeno-associated virus type 2-mediated gene transfer: correlation of tyrosine phosphorylation of the cellular single-stranded D sequence-binding protein with transgene expression in human cells in vitro and murine tissues in vivo. J. Virol. **72:**1593–1599.
20. **Qing, K., C. Mah, J. Hansen, S. Zhou, V. Dwarki, and A. Srivastava.** 1999. Human fibroblast growth factor receptor 1 is a co-receptor for infection by adeno-associated virus 2. Nat. Med. **5:**71–77.
21. **Schmid, S. L.** 1997. Clathrin-coated vesicle formation and protein sorting: an integrated process. Annu. Rev. Biochem. **66:**511–548.
22. **Summerford, C., J. S. Bartlett, and R. J. Samulski.** 1999. AlphaVbeta5 integrin: a co-receptor for adeno-associated virus type 2 infection. Nat. Med. **5:**78–82.
23. **Summerford, C., and R. J. Samulski.** 1998. Membrane-associated heparan sulfate proteoglycan is a receptor for adeno-associated virus type 2 virions. J. Virol. **72:**1438–1445.
24. **Urrutia, R., J. R. Henley, T. Cook, and M. A. McNiven.** 1997. The dynamins: redundant or distinct functions for an expanding family of related GTPases? Proc. Natl. Acad. Sci. USA **94:**377–384.
25. **van der Bliek, A. M., T. E. Redelmeier, H. Damke, E. J. Tisdale, E. M. Meyerowitz, and S. L. Schmid.** 1993. Mutations in human dynamin block an intermediate stage in coated vesicle formation. J. Cell Biol. **122:**553–563.
26. **Vieira, A. V., C. Lamaze, and S. L. Schmid.** 1996. Control of EGF receptor signaling by clathrin-mediated endocytosis. Science **274:**2086–2089.
27. **Wang, K., S. Huang, A. Kapoor-Munshi, and G. Nemerow.** 1998. Adenovirus internalization and infection require dynamin. J. Virol. **72:**3455–3458.
28. **Xiao, X., J. Li, and R. J. Samulski.** 1996. Efficient long-term gene transfer into muscle tissue of immunocompetent mice by adeno-associated virus vector. J. Virol. **70:**8098–8108.